



## Focus article

# Electrochemical reconstruction of a heavily corroded Tarentum hemiobolus silver coin: a study based on microfocus X-ray computed microtomography



Benedetto Bozzini <sup>a,\*</sup>, Alessandra Gianoncelli <sup>b</sup>, Claudio Mele <sup>a</sup>, Aldo Siciliano <sup>c</sup>,  
Lucia Mancini <sup>b</sup>

<sup>a</sup> Dipartimento di Ingegneria dell'Innovazione, Università del Salento, Via Monteroni, 73100 Lecce, Italy

<sup>b</sup> Elettra – Sincrotrone Trieste S.C.p.A., S.S. 14-km 163.5 in Area Science Park, 34149 Basovizza, Trieste, Italy

<sup>c</sup> Dipartimento di Beni Culturali, Università del Salento, Via Dalmazio Birago 64, 73100 Lecce, Italy

## ARTICLE INFO

## Article history:

Received 15 March 2014

Received in revised form

28 July 2014

Accepted 1 August 2014

Available online 11 August 2014

## Keywords:

X-ray computed microtomography

Electrochemistry

Electrodeposition

Coin legibility

Ag

AgCl

## ABSTRACT

In this paper we report on the electrochemical reconstruction of a Tarentum hemiobolus Ag coin, severely corroded in marine environment. As assessed by conventional analytical tools, most of the initially metallic Ag coin had been converted to AgCl by exposure to the aggressive coastal burial conditions. X-ray computed microtomography proved that only small portions of the artefact had preserved their metallic nature. Since the engraving was preserved partly in the corrosion product bulk and partly in the metallic rests, electrodeposition of Ag from the AgCl layer, under controlled conditions ensuring shape preservation, resulted in the reconstruction of the coin surface with full recovery of the original engraving. Such optimal electrodeposition conditions were identified by a combination of electrochemical and quasi-in situ X-ray microtomography experiments, carried out with artificially corroded engraved Ag wires. Microtomography of the reconstructed coin confirmed the compaction of the external Ag layer and disclosed that the central core of the coin still contains unconverted AgCl. The presence of such a mineralised core does not however impact the numismatic use of the coin and the safeguard of the original engraving.

© 2014 Elsevier Ltd. All rights reserved.

## 1. Introduction

Archaeological excavations carried out during 1977 in Saturo (ca. 10 km South-East of Taranto, Italy, Fig. 1. See [Supplementary Section 1](#)) have disclosed a sanctuary that has been in use since the middle of the 7th century B.C.. Since the second half of the subsequent century, the sanctuary was endowed with architectural structures and flourished until the end of the 3rd century B.C., when the site was abandoned after a fire (see [Supplementary Section 2](#)). In the *thesauròs* of the sanctuary over one thousand silver silver coins and two gold ones were found ([Rutter, 2001](#)), in addition to some precious golden artefacts (rings, earrings, needles) and a cameo bearing the inscription *Telephos*, the Homeric hero. Owing to coastal shallow burial exposure, characterised simultaneously by high oxygenation, humidity and chloride concentration, a notable fraction of the retrieved silver coins exhibits heavy

encrustations overlying the original metal volume. Among the few legible coins, several stem from Taranto, Thuri and Eraclea ([Siciliano, 2001](#)). At the moment, the *terminus post quem* for dating the treasure is the golden tarentine coin minted under Pyrrhus ([Siciliano et al., 2014](#)): of course, the possibility of deciphering the so far illegible silver coins is expected to provide valuable additional historical information.

In the present paper, we studied a *hemiobolus* minted in Taranto, dated ca. 280 B.C. – in any case earlier than 212 B.C. – displaying thick corrosion layers on both sides, hiding almost completely the original engraving. In similar cases, the original surface markings sometimes remain as a pseudomorph composed of corrosion products. In our case, the metallic remnants are severely embrittled and typically exhibit open cracks filled with corrosion products. As detailed later on, in the course of this study the investigated item was found to exhibit two crescents and four pellets on the obverse side and two crescents, pellets and “ΛΙ” inscription on the reverse one. The historical and artistic importance of these items calls for material protection and restoration. In the present investigation we

\* Corresponding author.

E-mail address: [benedetto.bozzini@unisalento.it](mailto:benedetto.bozzini@unisalento.it) (B. Bozzini).



**Fig. 1.** The promontory between Porto Pirrone and Porto Saturo bays. The Source Shrine is indicated by a red arrow. (For interpretation of the references to colour in this figure legend, the reader is referred to the web version of this article.)

developed two complementary approaches: (i) to map the residual engraving encoded either in metallic remnants or in the corrosion product layer by using the X-ray computed microtomography (mCT) technique; (ii) to reduce the oxidised metal present in the overlayer to the elemental state in order to transfer a significant part of the original engraving – preserved by the pseudomorphic corrosion products layer – back to the metal core.

As far as the encrustation composition and structure are concerned, chlorargyrite (Phase I), exhibiting an NaCl crystal structure, is the ordinary corrosion product of Ag and high-Ag alloys (Wanhill,

2003). As one can appreciate from thermodynamic data, summarised e.g. in a Pourbaix diagram (Fig. 2), chlorargyrite results from the oxidising properties of near-surface, aerated seawater and shallow land burials. In fact, under the action of oxygen, Ag oxidises in near-neutral aqueous environments forming a  $\text{Ag}_2\text{O}$  film, (Panel A), that becomes unstable in the presence of chlorides, in which case  $\text{AgCl}$  is the dominating corrosion product in a wide pH range (Panel B) (Thompson et al., 2000). For more details of the corrosion-product chemistry and structure of Ag in chloride environment, see Supplementary Section 3. The specific topic of Ag

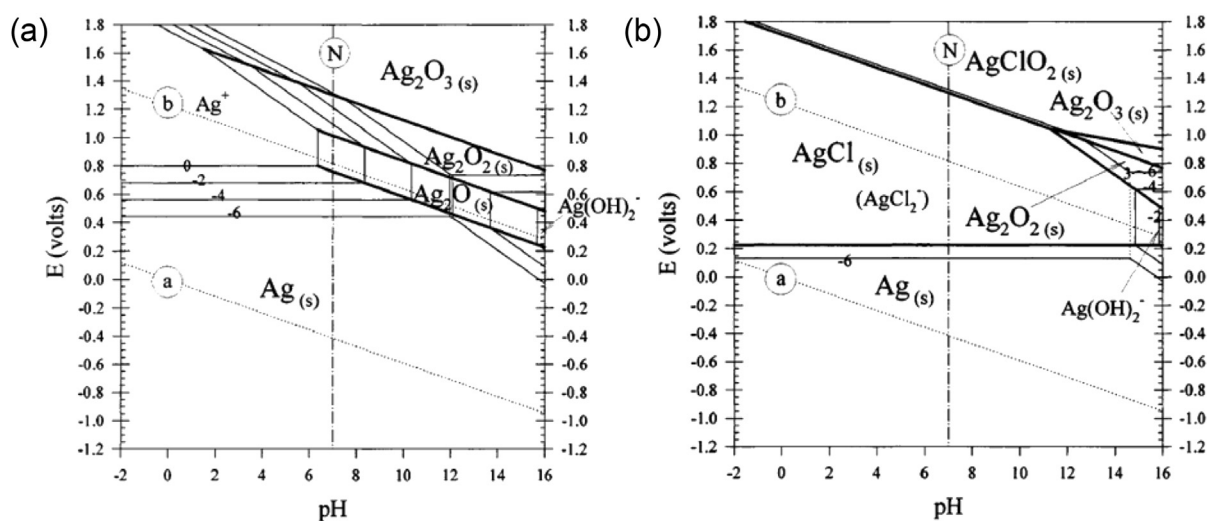


**Fig. 2.** Pourbaix diagrams at 25 °C for Ag in aqueous environments. (a) and (b) denote the hydrogen and oxygen lines, respectively. (N) corresponds to neutral pH. (A) In the absence of chlorides (concentrations of aqueous species range from  $1$  to  $10^{-6}$  M). (B) In the presence of 1 M chlorides (isoconcentration lines for  $\text{AgCl}_2^-$  and  $\text{Ag(OH)}_2^-$  are shown at  $10^{-6}$ ,  $10^{-4}$  and  $10^{-2}$  M). Adapted from Thompson et al., (2000).

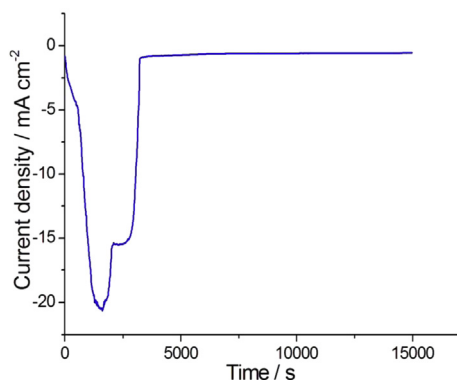


**Fig. 3.** Chronoamperometric curve corresponding to the reduction of a AgCl layer grown onto a Ag wire: electrolyte 0.1 M Na<sub>2</sub>SO<sub>4</sub>, −0.5 V vs. Ag/AgCl.

corrosion has received surprisingly limited attention in the literature and, in particular, material science aspects relevant to the protection of historic artefacts have hardly been covered (Giovannelli et al., 2005; McNeil and Little, 1992; Wanhill, 2003).

In this study we have characterised the composition and crystal structure of the coin under as-found conditions and after the potentiostatic reduction treatment. A brief review of the literature

on cognate electrochemical methods, used for the conservation of ancient metallic artefacts, is available in [Supplementary Section 4](#). In this context, it is worth stressing that our approach is entirely different from the traditional electrochemical treatment methods that can be briefly described as: (i) the compaction of objects, the mechanical properties of which are endangered by corrosion and (ii) the electrophoretic removal of potentially dangerous ionic compounds. In fact, our research consists in the actual electrodeposition of the metal from the corrosion products with the high geometrical precision allowed by the insolubility of AgCl: this way it is in principle possible to reconstruct the inscriptions of an initially illegible coin and not just to consolidate, clean or decontaminate it.

## 2. Materials and methods

### 2.1. Materials and electrochemical measurements

Neutral 0.8 M NaCl solutions were used for controlled corrosion experiments and neutral 0.1 M Na<sub>2</sub>SO<sub>4</sub> solutions for the cathodic treatments. These solutions were prepared with ultrapure water with resistivity of 18 MΩ cm from a Millipore Milli-Q system. Analytical-grade chemicals were employed. All experiments were

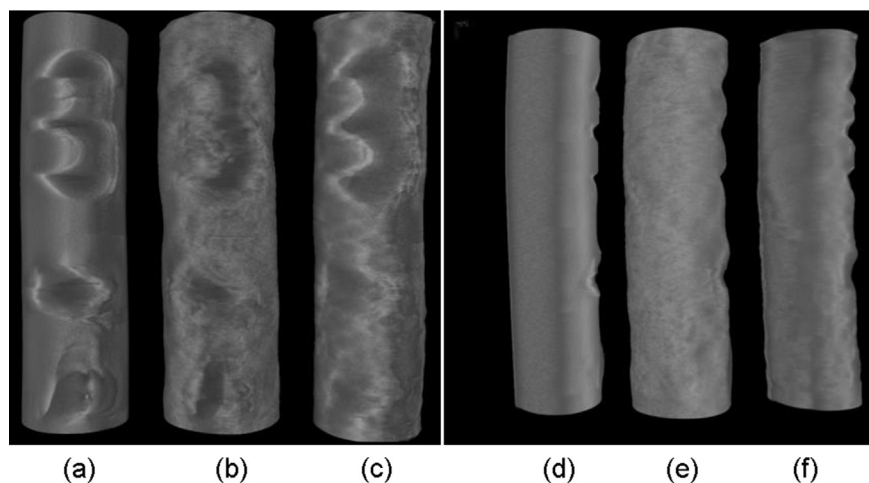


**Fig. 4.** Volume renderings obtained by X-ray mCT of: (a, d) original (2 mm diameter), (b, e) corroded and (c, f) reduced Ag wire sample. Panels (a)–(c) show frontal views of the engraved numbers, panels (d)–(f) depict side views.

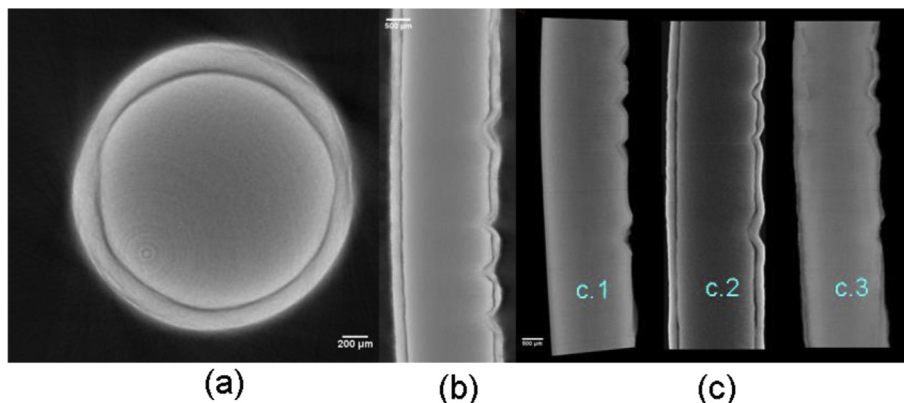


**Fig. 5.** Virtual sections, obtained by X-ray mCT, of the Ag wire: (a) XY (axial slice) of the Ag wire in corroded conditions; (b) higher magnification of the ZY plane of the Ag wire in corroded conditions (compare with Panel (c.2)); (c) ZY planes of pristine (c.1), corroded (c.2) and reduced (c.3) sample.





**Fig. 6.** Micrographs showing the comparison of the coin before (a) and after (b) the reduction process used for restoration. The reconstruction of the coins from the corrosion layer is well visible in these images revealing the original engraving.

carried out at room temperature. For more details on the electrochemical setups and experiments, see [Supplementary Section 5](#).

## 2.2. X-ray mCT analyses

The X-ray mCT experiments were performed at the TomoLab station, a custom-developed laboratory mCT system, built in collaboration with the University of Trieste, at the Elettra - Sincrotrone Trieste laboratory ([www.elettra.trieste.it](http://www.elettra.trieste.it)) in Basovizza (Italy). X-ray mCT is a non-destructive imaging method allowing the 3D reconstruction of an opaque object by illuminating it with X-rays in different directions (Kak and Slaney, 1988). The specimen is located between the X-ray source and the detector, and several radiographs (projections) of the object are recorded at different angular position of the object, during a full rotation of 360° degrees.

More instrumental and data-processing details on mCT are provided in [Supplementary Section 6](#).

## 2.3. Complementary analytics

In this research, the elemental composition was assessed by non-destructive X-ray fluorescence (XRF) spectroscopy with a Bruker M4 Tornado micro XRF spectrometer and the crystal structure was determined by X-ray diffraction (XRD) with an Ultima + Rigaku diffractometer, equipped with a Bragg–Brentano goniometer. Typical operating conditions were:  $\theta$ -2 $\theta$ , p.t. 3s, step 0.05, 40 kV, 20 mA. The employed radiation was unmonochromated Cu K $\alpha$ . Indexing of the patterns was accomplished using the PowderCell software ([www.bam.de](http://www.bam.de)), 3rd order cell parameters refinement was utilised. A detailed 3D morphological assessment has been based on microfocus X-ray mCT, disclosing microstructural features within the sample volume at the micron scale (Baker et al., 2012).

## 3. Results and discussion

### 3.1. Calibration studies with pure Ag wires

#### 3.1.1. Electrochemical oxidation/reduction

In order to assess the ability of cathodic reduction processes to restore the original morphology of a corroded Ag artefact partly mineralised to AgCl, we studied the controlled corrosion and reduction of engraved Ag wires. In the controlled corrosion process we formed a thick AgCl layer and in the subsequent cathodic treatment we reduced the adherent AgCl layer back to metallic Ag. On the basis of previous studies of ours (Bozzini et al., 2006, 2007) – that have provided insight into the relationships among electrokinetics, structure and morphology of AgCl formation –, we selected operating conditions ensuring the formation of thick (several tens of  $\mu\text{m}$ ), adherent AgCl layers, like the ones found in the heavily corroded ancient Ag coins. Details on this accelerated corrosion procedure are provided in [Supplementary Section 7](#). A series of reduction conditions was attempted, the details are omitted for brevity. The optimal condition was found to be potentiostatic treatment at  $-0.5$  V vs. Ag/AgCl. Conditions ensuring the

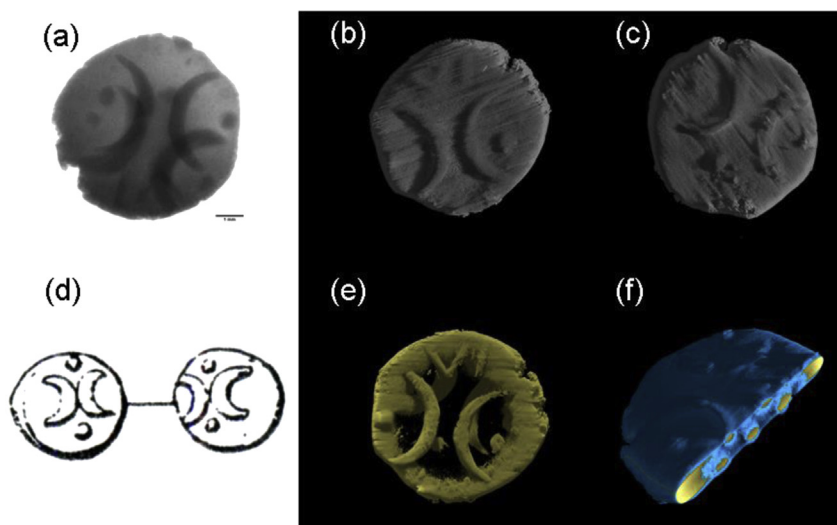


**Fig. 7.** X-ray images of the pristine coin sample shown in [Fig. 6](#), Panel (a). (a) X-ray radiograph; (b, c) Volume renderings obtained by X-ray mCT corresponding to faces I (b) and II (c); (d) schematic representation of the relevant type of Tarentum hemiobolus (#47) according to the classification of (Garrucci, 1885); (e) segmented image of the coin emphasizing only the Ag zones in yellow; (f) segmented image of the coin emphasizing both the Ag (yellow) and AgCl (blue) zones. (For interpretation of the references to colour in this figure legend, the reader is referred to the web version of this article.)

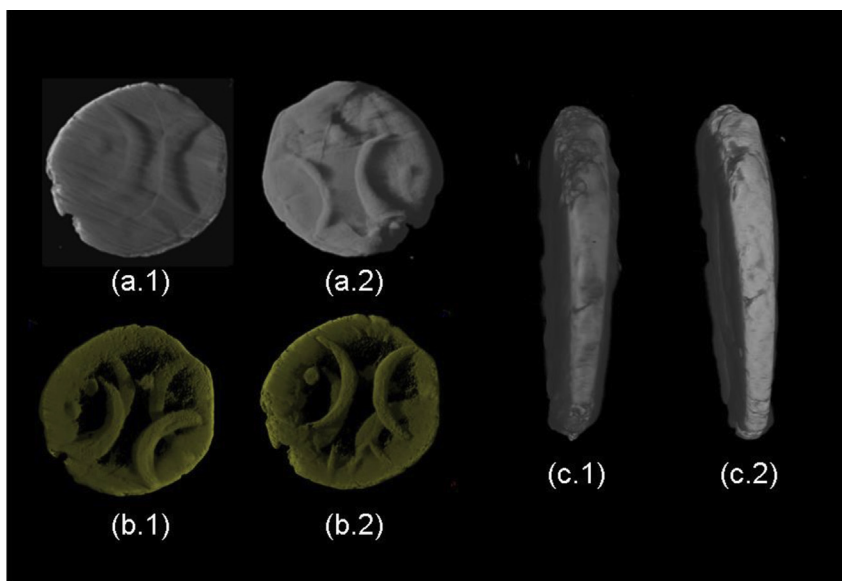


**Fig. 8.** Volume renderings obtained by X-ray mCT of the restored coin sample shown in Fig. 6, Panel (b). (a) Images corresponding to faces I (a.1) and II (a.2). (b) Segmented images of the coin, emphasising the metallic Ag zones in yellow (faces I (b.1) and II (b.2)). (c) Coin profiles before (c.1) and after (c.2) electrochemical reconstruction. (For interpretation of the references to colour in this figure legend, the reader is referred to the web version of this article.)

preservation of the morphology on the millimeter scale (relevant to conservation applications) essentially have to avoid excessively fast reduction, causing the detachment of the AgCl layer from the metallic substrate, and hydrogen evolution, leading to homogeneous reduction of the AgCl crust. A typical chronoamperometric curve corresponding to the reduction of previously corroded Ag wires is reported in Fig. 3. The time-dependence of the current density (c.d.) exhibits three periods: (i) initially the cathodic c.d. grows, until a maximum is reached, (ii) after which the c.d. progressively decreases until (iii) it attains a vanishing value. The initial growth corresponds to the establishment of steady-state ionic conductivity and the subsequent decrease to the progressive consumption of AgCl owing to its back-conversion to Ag. These cathodic conditions were applied to the ancient coin, enabling the reconstruction, detailed in the following Sections.

### 3.1.2. Quasi-in situ mCT imaging

A representative section of the cylindrical wire (height of 7.6 mm) was imaged by mCT in order to visualize the 3D micro-structure of the wire in three different conditions: (i) the original sample, (ii) the corroded state, (iii) after the reduction process: volume renderings are shown in Fig. 4. In Fig. 5 a reconstructed 2D axial slice (XY) (Panel (a)) and a 2D virtual section (ZY) (Panels (b, c)) of the corroded Ag wire are also shown. In Panel (c) virtual sections of the same sample in the pristine (c.1), corroded (c.2) and reduced (c.3) conditions pinpoint the formation and successive removal of the corrosion layer.

### 3.2. Electrochemical reconstruction of the ancient coin

The treated coin was characterised, in pristine conditions and after electrochemical reconstruction, by XRF, mCT and XRD, as detailed below.

#### 3.2.1. Optical and mCT imaging of the ancient coin in as-found condition and after electrochemical reconstruction

In Fig. 6 we report micrographs of both sides of the investigated coin in as-found (a) and electrochemically reconstructed (b) conditions. The reconstruction of the metallic surface and of the coin

engravings from the corrosion product layer is evident. In Fig. 7 we show a selection of X-ray images of the coin in as-found condition: the conversion of a large fraction of the original metal into corrosion products can be clearly assessed. Moreover, the original engraving – that is almost entirely inaccessible by visual inspection (Fig. 6a) – is now evident on both surfaces of the coin by using either X-ray microradiography (Panel (a)) or volume renderings (Panels (b, c)). In order to discriminate between the two principal phases present in the sample, a segmentation process – detailed in Supplementary Section 8 – was applied to the reconstructed volumes.

In Fig. 8, Panels (a.1) and (a.2), we report the volume renderings and the segmented 3D images of the two faces of the coin after electrochemical reconstruction. In Panel (c) a comparison of the coin profile before (c.1) and after (c.2) the electrochemical process is also displayed. The densification of the coin surface (Panels (a) and (c.1)) – ensuring a notable improvement in the conservation

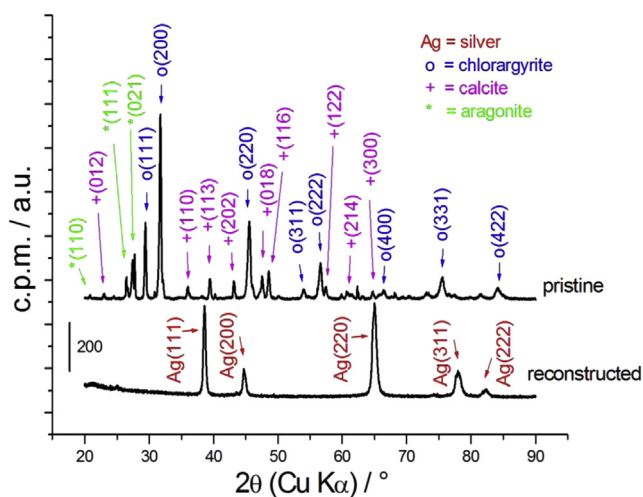


**Fig. 9.** X-ray diffractogram of the coin before and after the electrochemical reconstruction treatment.

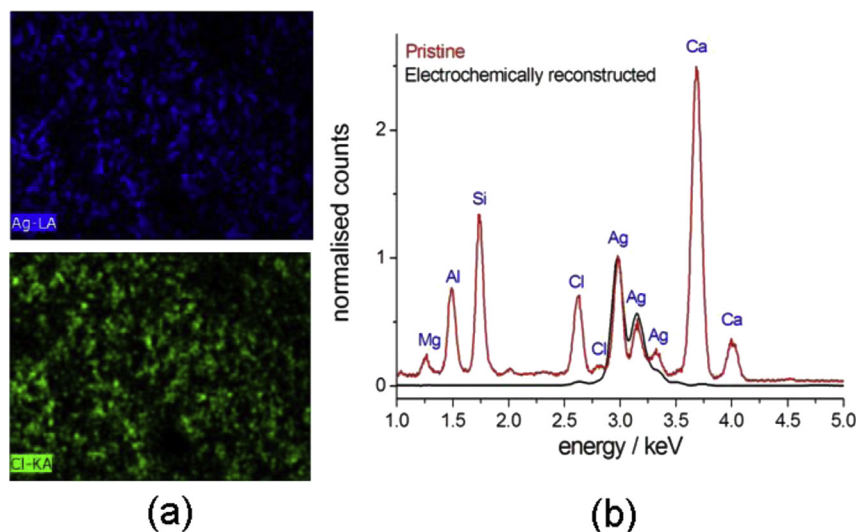


Fig. 10. (a) XRF maps of Ag and Cl for the pristine coin. (b) XRF spectra of the coin in pristine and electrochemically reconstructed forms.

and historical use of the coin – is evident even though the corroded core is not entirely converted to metal (Panels (b.1) and (b.2)), as expected from the prevailing current density distribution, that insulates the core after completion of the external metallic shell.

### 3.2.2. XRD and X-ray fluorescence analyses of the ancient coin in as-found and electrochemically reconstructed conditions

X-ray diffractograms measured before and after the electrochemical treatment are reported in Fig. 9. The as-found coin exhibits a single-phase structure of the corrosion product, consisting of pure AgCl(I) (chlorargyrite); in addition to the corrosion product reflections, calcite and aragonite peaks were found, deriving from the burial soil. It is worth noting that no peaks corresponding to metallic Ag were detected in as-found condition, because the amount of residual Ag<sup>0</sup> is very limited and the metal fragments are embedded into the AgCl bulk (see also the mCT results reported in Section 3.2.1). After the electrochemical treatment, the XRD structure of the coin is pure Ag: all detectable AgCl is converted back to Ag<sup>0</sup> and the soil contaminants are released to the treatment solution.

In Fig. 10a we report XRF maps of the coin in pristine conditions, exhibiting large and homogeneously distributed amounts of Ag and Cl. The XRF spectra (Fig. 10b) from the as-found coin show the presence of large amounts of Ag and Cl, together with soil components (Mg, Al, Si), while after electrochemical reconstruction the analysed surface essentially consists of Ag with just minor traces of Cl.

## 4. Conclusions

In this paper we have characterised a hemiobolus recovered from the Saturo hoard, that has undergone serious coastal corrosion, resulting in almost complete loss of the original engraving and nearly full conversion of the artefact into AgCl. Micro-computed tomography (mCT) of the coin in as-found condition revealed that only small, internal fractions of the volume had preserved their metallic nature; nevertheless, the original engraving resulted to be preserved, encoded in the corrosion product bulk. Since cathodic electrochemistry in principle gives the possibility of back-converting AgCl to Ag, we endeavoured to carry out this process in a way that could allow the recovery of the original engraving, by shape-preserving electrodeposition. The optimal electrodeposition

conditions were preliminarily checked by reconstructing a series of test images engraved on modern Ag wires: these tests were carried out by combining suitable dynamic electrochemical measurements with quasi-in situ mCT. Successful reconstruction of the corroded coin was assessed by visual inspection, optical micrography, XRD and XRF, proving complete reduction of the portions of the coin accessible to analysis. mCT revealed that the actually reconstructed volume is in fact a shell, while the electrochemically screened coin core still contains AgCl. Notwithstanding the quantitatively incomplete backconversion of the whole coin bulk, we reckon that our treatment is fully satisfactory in that: (i) the coin has been returned to the original appearance and is fully accessible for numismatic studies and museum exhibition; (ii) preservation is fully ensured, since – at variance with other systems, such as bronze disease – the residual corrosion product content is not liable to trigger corrosion of the metallic shell; (iii) the mechanical properties of the coin have been improved to a level that the item can be handled essentially as if it were fully metallic. Moreover, it is worth noting that the traditional cleaning and restoration approaches cannot be employed with this type of degradation and several attempts have resulted in the utter destruction of the corroded coins. Future investigations are aimed at: (i) improving the current-density distribution of the process in a way that the reduction process will proceed from one side of the coin inwards, eventually reaching the other side, instead of reducing the whole surface of the object thereby excluding the internal parts from access of the applied electric field, as we in fact did in the present study; (ii) applying systematically the approach to the rich collection of more than 1100 corroded ancient Ag coins from the Saturo hoard, currently stored in the Museo Nazionale Archeologico (National Archaeological Museum) in Taranto, that have yet not been formally classified and described in the open literature.

## Acknowledgments

High-standard technical support by Dr. Nicola Sodini (Elettra) is gratefully acknowledged.

## Appendix A. Supplementary data

Supplementary data related to this article can be found at <http://dx.doi.org/10.1016/j.jas.2014.08.002>.

## References

- Baker, D.R., Mancini, L., Polacci, M., Higgins, M., Gualda, G.A.R., Hill, R., Rivers, M., 2012. An introduction to the application of x-ray microtomography to the three-dimensional study of igneous rocks. *Lithos* 148, 262–276.
- Bozzini, B., Giovannelli, G., Mele, C., Brunella, F., Goidanich, S., Pedferri, P., 2006. An investigation into the corrosion of Ag coins from the Greek colonies of Southern Italy. Part I: an in situ FT-IR and ERS investigation of the behaviour of Ag in contact with aqueous solutions containing 4-cyanopyridine. *Corros. Sci.* 48, 193–208.
- Bozzini, B., Giovannelli, G., Mele, C., 2007. Electrochemical dynamics and structure of the Ag/AgCl interface in chloride-containing aqueous solutions. *Surf. Coat. Technol.* 201, 4619–4627.
- Garrucci, R., 1885. *Le monete dell'Italia antica. Coi tipi del cav. V. Salviucci*. Roma.
- Giovannelli, G., Natali, S., Bozzini, B., Siciliano, A., Sarcinelli, G., Vitale, R., 2005. Microstructural characterisation of early western Greek incuse Coins. *Archaeometry* 47, 817–833.
- Kak, A.C., Slaney, M., 1988. *Principles of Computerized Tomographic Imaging*. IEEE Press electronic copy. <http://www.slaney.org/pct/pct-toc.html>.
- McNeil, M.B., Little, B.J., 1992. Corrosion mechanisms for copper and silver objects in near-surface environments. *J. Am. Inst. Conserv.* 31, 355–366.
- Rutter, N.K., 2001. *Historia Numorum – Italy*. British Museum Press, London.
- Siciliano, A., 2001. La circolazione monetale. In: *Atti del XLI Convegno di Studi sulla Magna Grecia: Taranto e il Mediterraneo*. Istituto per la storia e l'archeologia della Magna Grecia, Taranto, pp. 483–518.
- Siciliano, A., Bozzini, B., Buccolieri, G., Gianoncelli, A., Mancini, L., Manno, D.E., Serra, A., 2014. Il ruolo dell'Università tra ricerca e tutela. *Notiziario del Portale Numismatico dello Stato*, 4, pp. 38–52. <http://www.numismaticadellostato.it/web/pns/notiziario>.
- Thompson, W.T., Kaye, M.H., Bale, C.W., Pelton, A.D., 2000. Pourbaix diagrams for multielement systems. In: Revie, R.W. (Ed.), *Uhlig's Corrosion Handbook*, second ed. John Wiley and Sons, N.Y, pp. 125–136. Chapter 7.
- Wanhill, R.J.H., 2003. Brittle archaeological silver: a fracture mechanisms and mechanics assessment. *Archaeometry* 45, 625–636.